

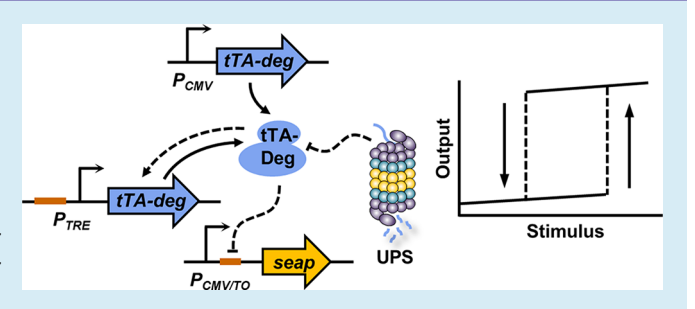
Hysteretic Genetic Circuit for Detection of Proteasomal Degradation in Mammalian Cells

Yimeng Zeng,[†] Bachhav Bhagyashree,[†] Wenting Zhao,[†] Tram Nguyen,[†] and Laura Segatori*,^{†,‡,§}

[†]Department of Chemical and Biomolecular Engineering, [‡]Department of Bioengineering, and [§]Department of Biosciences, Rice University, Houston, Texas 77005, United States

Supporting Information

ABSTRACT: Synthetic hysteretic mammalian gene circuits generating sustained cellular responses to transient perturbations provide important tools to investigate complex cellular behaviors and reprogram cells for a variety of applications, ranging from protein production to cell fate decisions. The design rules of synthetic gene circuits with controlled hysteretic behaviors, however, remain uncharacterized. To identify the criteria for achieving predictable control of hysteresis, we built a genetic circuit for detection of proteasomal degradation (Hys-Deg). The Hys-Deg circuit is



based on a tetracycline-controlled transactivator (tTA) variant engineered to interface with the ubiquitin proteasome system (UPS). The tTA variant activates its own expression, generating a positive feedback loop that is triggered by expression of another tTA gene that is constitutively regulated. Guided by predictive modeling, we characterized the hysteretic response of the Hys-Deg circuit. We demonstrated that control of the hysteretic response is achieved by modulating the ratio of expression of constitutive to inducible tTA. We also showed that the system can be finely tuned through dosage of the inducer tetracycline to calibrate the circuit for detection of the desired levels of UPS activation. This study establishes the design rules for building a hysteretic genetic circuit with an autoregulatory feedback loop and provides a synthetic memory module that could be easily integrated into regulatory gene networks to study and engineer complex cellular behaviors.

KEYWORDS: hysteresis, genetic circuit, protein degradation, mammalian cell, positive feedback, predictive modeling

ngineering mammalian cells holds great potential for the design of cell-based technologies, ranging from the design of in vitro model systems to study human diseases to the development of cell-based therapies for in vivo implantation and technology platforms for biopharmaceutical manufacturing.^{1,2} Cell engineering requires the use of tools that provide precise control over complex gene networks and metabolic pathways to achieve, for instance, controlled production of recombinant proteins or metabolites,^{3–7} cell differentiation,^{8,9} or cell reprogramming. 10,11 Cell engineering strategies have historically capitalized on the use of regulatory parts orthogonal to the cellular components. These synthetic or nature inspired biological parts can be organized into networks and combined to generate network topologies with specialized behaviors, resulting in the design of "programmable" cells and organisms.^{8,12} Engineering cells using programmable genetic networks allows precise and dynamic control over gene expression and cell development, 13,14 which is required to create model systems of complex physiological processes, 15,16 design stimulus-responsive biosensors, 11,17,18 and develop cell factories for the production of valuable biomolecules. 19

One of the main challenges of cellular reprogramming is associated with the innate ability of mammalian cells to attenuate perturbations in cell physiology. 20,21 Attenuation is achieved through a highly sophisticated quality control system, which typically induces a cellular response aimed at restoring homeostasis. The nature of mammalian cells to attenuate perturbations points to the need for programmable genetic devices that can record cellular events and generate a signal that provides cellular memory^{22,23} of an otherwise transient change in cell physiology. A genetic device with cellular memory produces detectable signals that are sustained even after attenuation of the biological phenomenon generating the signal, which often occurs due to the sophisticated homeostatic mechanisms of mammalian cells. In such memory devices, the strength of stimulus required to evoke a functional reaction switching the system from the default state to an induced state is typically higher than that of the stimulus required to maintain the system in the induced state.²⁴ This property, referred to as hysteresis, allows the genetic circuit to maintain in the induced state after decrease or removal of the stimulus, and thus confers cells the ability to generate self-sustainable responses to transient perturbations.

Hysteresis can be effectively achieved utilizing a positive feedback loop that is robust enough to generate a bistable genetic switch.^{25,26} In a genetic circuit, positive feedback results from placing the expression of a gene under its own

Received: February 20, 2019 Published: August 15, 2019



control directly, via autoregulation,²⁷ or indirectly, via mutual inhibition.²⁸ Positive feedback loops play an important role in both natural and synthetic gene regulatory networks.^{27–31} Natural hysteretic systems based on positive feedback loops are essential for a variety of cellular processes governing the behaviors of mammalian cells, such as cell cycle and cell differentiation.^{8,9} In addition, synthetic gene circuits containing engineered positive feedback loops have been used as genetic amplifiers for enhancement of gene expression.^{32–34} Despite the extensive efforts devoted to the design of complex hysteretic systems,^{25,35,36} the design rules of the self-activation based hysteresis remain uncharacterized. Previous studies have demonstrated circuit topologies that display hysteresis;^{37,38} a quantitative interpretation of hysteretic behaviors and the criteria for regulating hysteresis, however, have not been defined.

In this study, we report the development of a hysteretic system for detecting activation of the ubiquitin proteasome system (UPS). The UPS is an important cellular machinery responsible for the disposal of misfolded and damaged proteins in eukaryotic cells.³⁹ Upregulation of proteasomal degradation was reported to promote clearance of misfolded proteins and toxic protein aggregates, implicating the UPS as a potential therapeutic target for the treatment of protein misfolding diseases. 40-42 However, current technologies for investigating proteasomal degradation in living cells and in vivo are typically based on reporter proteins engineered to function as UPS substrates and generate an inverse correlation between enhancement of proteasomal degradation output signal, 43,44 and are thus not ideal for high-throughput applications. To engineer a cellular device that links enhancement of proteasomal degradation to an increase in output signal and also provides a memory of transient changes in UPS activity, we designed a genetic circuit based on a self-activation loop that interfaces with the proteasomal degradation machinery. Specifically, the self-activation loop consists of the tetracyclinecontrolled transactivator (tTA), the expression of which is controlled by the tetracycline-inducible promoter. Selfactivation of the tTA expression is triggered by the expression of another tTA-encoding gene controlled by a constitutive promoter. Expression of the reporter of the circuit, the secreted embryonic alkaline phosphatase (SEAP), is repressed by tTA. tTA, in this circuit, has been engineered to function as a substrate of the UPS by fusion to a degron tag. Activation of UPS results in degradation of the degron-tagged tTA. Predictive modeling was used to investigate the design rules for building this hysteretic genetic circuit. We demonstrate that the system exhibits tunable hysteretic response upon modulation of the ratio of constitutively expressed to inducible tTA, thereby providing design rules for achieving hysteresis with a self-activation loop. We also show that this genetic circuit converts enhancement of UPS activity into an extracellular output signal and can be finely tuned using tetracycline to detect desired levels of proteasomal degradation.

RESULTS

Design of the Hys-Deg Circuit. To investigate the design rules for establishing a hysteretic system that can detect proteasomal degradation, we constructed a genetic circuit containing a self-activation loop based on the inducible Tet regulatory system, which is a well characterized and widely used regulatory system in eukaryotic cells.^{34,45–47} The self-

activation loop was implemented by the tetracycline-controlled tTA, which consists of the tetracycline repressor (TetR) fused to the C-terminal acidic domain of virion protein 16 (VP16), a transcriptional activator domain of herpes simplex virus. ⁴⁵ tTA can function as a repressor when bound to the tetracycline operator (TO) placed downstream of the TATA box of a promoter, ⁴⁶ and can also function as an activator when bound to TO placed upstream of a minimal promoter. ⁴⁵

The architecture of this circuit (Hys-Deg) is as follows (Figure 1). Self-amplification of tTA expression was driven by

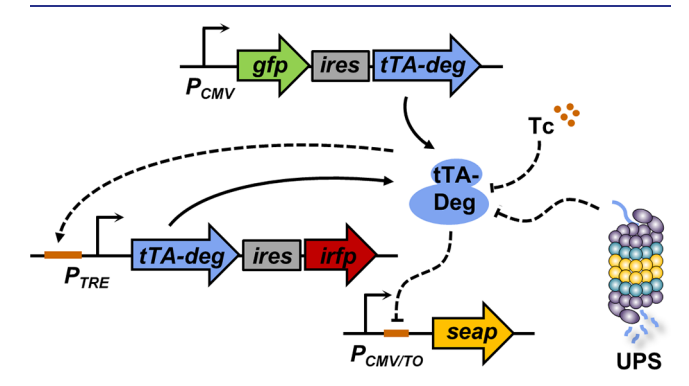


Figure 1. Schematic illustration of the Hys-Deg system. The tTA variant tTA-Deg is expressed from two cassettes, one controlled by a constitutive *CMV* promoter and one controlled by an inducible *TRE* promoter. The constitutive and inducible expressions of tTA-Deg are linked to the expression of GFP and iRFP, respectively. tTA-Deg activates its own expression by binding to the tetracycline operator (TO) in the *TRE* promoter and represses the expression of secreted embryonic alkaline phosphatase (SEAP) by binding to TO in the *CMV/TO* promoter. The addition of tetracycline (Tc) or enhancement of UPS activity blocks self-activation of tTA-Deg and activates SEAP expression.

an inducible TRE promoter, which consists of seven repeats of TO upstream of a minimal CMV promoter. 46 By binding to the operators in the TRE promoter, tTA activates its own expression. The self-amplification loop is triggered by expression of another tTA cassette that is expressed constitutively under the control of the CMV promoter. The expression of tTA under the control of the constitutive CMV promoter and that of tTA under the control of the inducible TRE promoter were linked to the expression of the green fluorescent protein (GFP) and the near-infrared fluorescent protein (iRFP), respectively, through the use of internal ribosome entry site (IRES) sequences placed between the gene encoding tTA and the gene encoding the fluorescent reporter in each construct.⁴⁸ Expression of the SEAP was controlled by the tetracycline-inducible CMV/TO promoter. The binding of tTA to the operators in the CMV/TO promoter results in repression of SEAP expression. tTA, in this circuit, was engineered as a substrate of proteasomal degradation by fusion to the ODC degron tag, which is the 37 amino acid carboxyterminal sequence of ornithine decarboxylase (generating tTA-Deg).49,50

Proteasomal degradation of tTA-Deg results in expression of SEAP, which thus provides a reporter of UPS activity. SEAP production is alternatively induced by tetracycline, which displaces tTA from the operator, ⁴⁵ preventing self-amplification of tTA. The Hys-Deg circuit generates a correlation between enhancement of proteasomal degradation (input) and SEAP expression (output). The addition of tetracycline

enables simulating UPS activation quantitatively and can also be used to finely tune the circuit sensitivity to UPS activation.

Predictive Modeling and Design Rules of the Hys-Deg Circuit. To define the criteria for creating a synthetic gene circuit with hysteretic output, we developed a mathematical model based on ordinary differential equations that simulates the behavior of the Hys-Deg circuit. In this model, tTA expression was determined by the rates of protein synthesis, degradation, and dilution arising from cell division,³⁴ whereas the production of SEAP was determined by the rates of protein synthesis and degradation, and is proportional to the cell count.⁵¹ The model was also based on the assumptions that transcription is fast compared to translation, and tTA dimerization is fast compared to dissociation and degradation.⁵² The states of promoters in which the transcription factors are bound to single operator sequences were neglected.³⁴ The degradation of all proteins and dynamics of translation were considered linear. 52 We also assumed UPS activation to have negligible effect on the degradation rate of highly stable proteins, namely, GFP, 53 iRFP, 54 and SEAP, 51 compared to the ODC-tagged tTA variant.³⁴ Since tetracycline diffusion through the cell membrane is much more rapid than tTA and SEAP expression, 55 the rate of tetracycline uptake and degradation were neglected and intracellular tetracycline concentration was treated as a constant.

The rate of synthesis of tTA was determined by the rate of tTA synthesis controlled by the constitutive CMV promoter and the rate of tTA synthesis controlled by the inducible TRE promoter, as described in the Materials and Methods. The rate of tTA synthesis controlled by the TRE promoter was modeled as following a Hill function, 56 including basal activity to account for leakiness. The rate of synthesis of SEAP was modeled as following a Hill function, including basal activity to describe the leakiness of the CMV/TO promoter. The Hill function describing protein synthesis was derived as a function of tetracycline concentration and to also include residual binding of tetracycline-bound tTA to TO as previously reported.³⁴ The rates of protein synthesis of unbound CMV/ TO promoters and bound TRE promoters were considered to be equal to the promoter's maximal synthesis rate, whereas the rates of protein synthesis of bound CMV/TO promoters and unbound TRE promoters were considered to be zero. The parameter values are provided in Supplementary Table 1.

We defined the "OFF" and "ON" states of the system in terms of SEAP expression: when SEAP expression is repressed (high tTA expression), the system is "OFF"; when SEAP expression is derepressed (low tTA expression), the system is "ON". The predictive model showed that SEAP production increased as a function of UPS activity, which was modeled by decreasing the half-life of tTA (Figure 2), confirming that the Hys-Deg circuit is a sensor of proteasomal degradation. A threshold of UPS activity was observed to control the OFF-to-ON switch (Figure 2). The addition of tetracycline lowered the threshold of UPS activity (and thus increased the threshold of tTA half-life) needed to switch the circuit from the OFF-to-ON state (Figure 2). These findings suggest that the Hys-Deg circuit can be finely tuned to detect the desired levels of UPS activation through the addition of tetracycline to the culture medium.

We next investigated the effect of tTA synthesis from the constitutive and inducible promoters on the circuit's hysteresis. Predictive modeling revealed that the width of the hysteretic region, which is defined as the range of tetracycline dosage

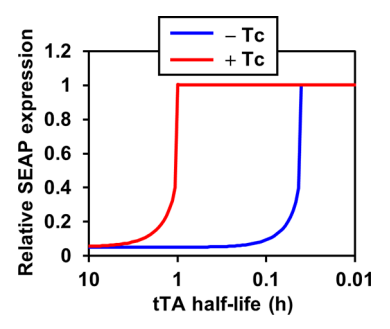
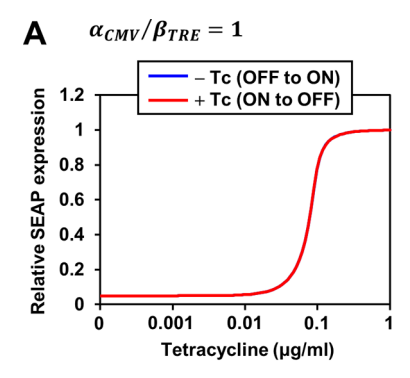
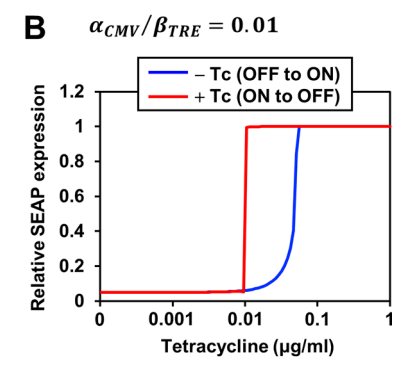


Figure 2. Model prediction of SEAP expression as a function of UPS activity. SEAP expression of the Hys-Deg circuit as a function of tTA half-life in the presence (0.02 $\mu g/mL$) and absence of tetracycline. Relative SEAP expression values were calculated by normalizing SEAP concentrations to those obtained in the presence of high concentration of tetracycline (1 $\mu g/mL$).

between the threshold of tetracycline corresponding to the ON-to-OFF switch and the threshold of tetracycline corresponding to the OFF-to-ON switch, is a function of the ratio of the rate of tTA synthesis driven by the constitutive CMV promoter (α_{CMV}) to the rate of tTA synthesis driven by the inducible *TRE* promoter (β_{TRE}) (Figure 3). Specifically, the hysteretic region increases as the ratio of constitutive to inducible synthesis rate, α_{CMV}/β_{TRE} , decreases. We simulated SEAP expression as a function of tetracycline concentration $(0-1 \mu g/mL)$ at different α_{CMV}/β_{TRE} ratios, namely high $(\alpha_{CMV}/\beta_{TRE} = 1)$, intermediate $(\alpha_{CMV}/\beta_{TRE} = 0.01)$, and low $(\alpha_{CMV}/\beta_{TRE} = 0.0001)$. When the system was preset at the OFF state (0 μ g/mL tetracycline), SEAP expression was predicted to increase as a function of tetracycline concentration, and to be completely turned ON when tetracycline concentration reaches an intermediate level ($\sim 0.05-0.2 \mu g/$ mL) at all α_{CMV}/β_{TRE} ratios. When the system was preset at the ON state (1 μ g/mL tetracycline), the threshold of tetracycline concentration that switches SEAP expression OFF was the same as the threshold of tetracycline concentration that switches SEAP expression from OFF to ON in the circuit presenting a high $\alpha_{\rm CMV}/\beta_{\rm TRE}$ ratio $(\alpha_{\rm CMV}/\beta_{\rm TRE}=1)$ (0.2 $\mu{\rm g}/$ mL, Figure 3A). However, the tetracycline concentration needed to switch SEAP expression OFF in the circuits presenting intermediate ($\alpha_{CMV}/\beta_{TRE} = 0.01$) and low ($\alpha_{CMV}/\beta_{TRE} = 0.0001$) α_{CMV}/β_{TRE} ratios decreased ($\sim 0.01~\mu g/mL$, Figure 3B; ~0.001 μ g/mL, Figure 3C). As α_{CMV}/β_{TRE} decreased, the response of the Hys-Deg circuit to tetracycline dosage shifted from a graded (Figure 3A) to hysteretic response (Figure 3B,C), which is characterized by a higher tetracycline concentration required to switch the system from the OFF to the ON state than from ON to OFF state. Moreover, the difference between the threshold of tetracycline corresponding to ON-to-OFF switch and the threshold of tetracycline corresponding to OFF-to-ON switch increased from ~5-fold (at intermediate α_{CMV}/β_{TRE}) to ~50-fold (at low α_{CMV}/β_{TRE}) as α_{CMV}/β_{TRE} decreased (Figure 3B,C). Bifurcation analyses describing the paths followed by the Hys-Deg system based on tetracycline concentration as bifurcation parameter also predicted that intermediate and low α_{CMV}/β_{TRE} result in bistability (Supplementary file Figure S1). In summary, the mathematical model predicts that the Hys-Deg circuit exhibits a tunable hysteretic response that can be modulated by controlling the ratio of synthesis of constitutively expressed to inducible tTA.





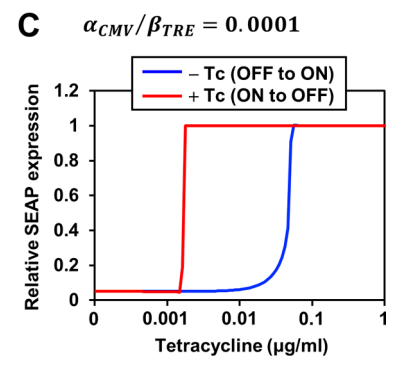


Figure 3. Model prediction of SEAP expression as a function of tetracycline dosage for different α_{CMV}/β_{TRE} ratios. SEAP expression of the Hys-Deg circuit presenting (A) $\alpha_{CMV}/\beta_{TRE} = 1$, (B) $\alpha_{CMV}/\beta_{TRE} = 0.01$, (C) $\alpha_{CMV}/\beta_{TRE} = 0.0001$ as a function of tetracycline concentration, preset at the ON (red) and OFF (blue) state. The OFF and ON state correspond to the steady states of the system in the absence of tetracycline (-Tc) and in the presence of high tetracycline (+Tc, 1 μ g/mL). Relative SEAP expression values were calculated by normalizing SEAP expression levels obtained when tTA expression reaches steady state in the presence of increasing tetracycline concentrations to those obtained in the presence of a high concentration of tetracycline (1 μ g/mL).

Implementation of the Hys-Deg Circuit as a Sensor of Proteasomal Degradation. To experimentally verify that the Hys-Deg system functions as predicted by the mathematical model, we constructed a cell line expressing the Hys-Deg circuit. A parental cell line expressing SEAP was first generated by transfecting HEK293T cells for the expression of SEAP under the control of the CMV/TO promoter (pTO_SEAP) and selecting a stable, monoclonal population presenting moderate SEAP activity (a clone displaying SEAP activity equal to the average SEAP activity of 30 clones screened) (Figure S2). To achieve precise control over the ratio of constitutively expressed to inducible tTA, the

cassettes encoding *tTA* under the control of *CMV* and *TRE* promoters were cloned into two separate lentiviral vectors. The parental SEAP expressing cell line was sequentially transduced using lentiviral vectors encoding the constitutively expressed tTA (pLenti CMV_tTA) and self-activated tTA (pLenti TRE_tTA), and selected in bulk to obtain a polyclonal population stably expressing the Hys-Deg circuit. The ratio of constitutive to inducible tTA was modulated by isolating monoclonal populations expressing different levels of GFP and iRFP (Figure S3), which serve as reporters of constitutively expressed and inducible tTA driven by the *CMV* and *TRE* promoters, respectively. We isolated a clone presenting a high GFP to iRFP ratio (HEK293T/Hys#1, Figure 4A), which is

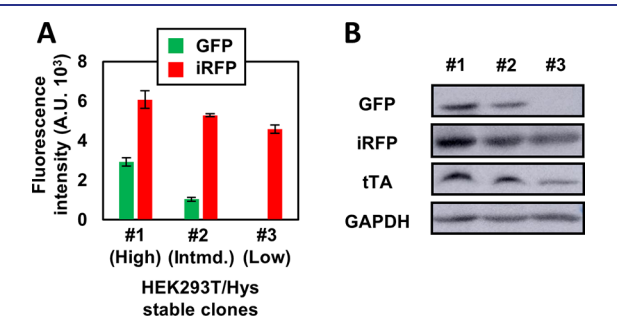


Figure 4. Modulation of the ratio of constitutively expressed to inducible tTA. (A) Flow cytometry analyses of HEK293T cells stably expressing the Hys-Deg circuit presenting high (HEK293T/Hys#1), intermediate (HEK293T/Hys#2), and low (HEK293T/Hys#3) ratios of constitutive to inducible tTA (α_{CMV}/β_{TRE}). Data are reported in arbitrary units (A.U.) and presented as mean \pm s.d. ($n \ge 3$, p < 0.001, two tailed t test). (B) Western blot analyses of GFP, iRFP, and tTA. GAPDH was used as a loading control.

indicative of a high ratio of expression of constitutive to inducible tTA, corresponding to a high α_{CMV}/β_{TRE} ratio. We also isolated a clone displaying an intermediate GFP to iRFP ratio (HEK293T/Hys#2), which is indicative of an intermediate $\alpha_{\rm CMV}/\beta_{\rm TRE}$ ratio, and a clone displaying a low GFP to iRFP ratio (HEK293T/Hys#3), which is indicative of a low α_{CMV}/β_{TRE} ratio (Figure 4A, p < 0.001). The GFP fluorescence intensity of HEK293T/Hys#3 cells (low α_{CMV}/β_{TRE} ratio) was comparable to that of the parental (nontransduced) cell line (Figure S4A). Analyses of GFP mRNA levels of HEK293T/ Hys#1, HEK293T/Hys#2, and HEK293T/Hys#3 confirmed integration of the constitutively expressed tTA cassette (Figure S4B and S4C). The iRFP fluorescence signal of the three cell lines decreased as $\alpha_{\text{CMV}}/\beta_{\text{TRE}}$ decreased, suggesting that the differences in the TRE promoter activity arise from different total amounts of tTA. To confirm that the GFP and iRFP signals measured by flow cytometry are accurate measurements of tTA expression levels driven by the CMV and TRE promoters, we analyzed GFP, iRFP, and tTA protein levels. Western blot analyses showed that GFP and iRFP protein levels were consistent with the fluorescence intensity measurements, and tTA protein levels decreased as a function of the GFP protein level (Figure 4B), suggesting that the ratio of GFP to iRFP fluorescence is a reliable indicator of the ratio of constitutive to inducible tTA synthesis rate α_{CMV}/β_{TRE} .

To evaluate whether the Hys-Deg circuit can detect proteasomal degradation, we monitored SEAP activity upon genetic activation of the UPS, which was achieved by overexpressing the proteasome activator subunit PA287. HEK293T/Hys cells were transfected for the expression of

PA28 γ , and treated with tetracycline to tune the detection of proteasomal degradation as guided by the model prediction. Overexpression of PA28 γ did not significantly affect the SEAP activity of cells cultured in the absence of tetracycline, suggesting that the level of UPS activation achieved did not reach the threshold needed to switch the system from OFF to ON. However, the addition of tetracycline to cells overexpressing PA28 γ resulted in an increase in SEAP activity ranging from 1.6- to 2.1-fold (Figure 5, *p < 0.05, **p < 0.01).

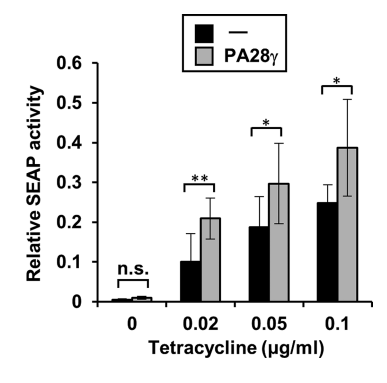


Figure 5. Quantification of proteasomal degradation using the Hys-Deg circuit. SEAP activity of HEK293T/Hys#1 cells transiently transfected for the expression of PA28 γ or with a control plasmid lacking the PA28 gene (–) and cultured in the absence or presence of tetracycline. Relative SEAP activity values were calculated by normalizing the SEAP activity of each sample to that of cells treated with 1 μ g/mL tetracycline (maximum SEAP activity). Data are presented as mean \pm s.d. ($n \ge 3$, *p < 0.05, **p < 0.01, two tailed t test).

These results are consistent with the predictions of the mathematical model and suggest that the system can be modulated with tetracycline to lower the threshold of UPS activity corresponding to the OFF-to-ON switch. The fold change of SEAP activity detected upon overexpression of PA28y decreased as tetracycline dosage increased (Figure 5). This result is due to the ultrasensitivity of the TRE promoter, which displays sharp changes in activity with small changes in tetracycline concentration at intermediate tetracycline concentrations, and becomes saturated at high tetracycline concentrations.²⁵ Culturing conditions corresponding to the highest fold change in SEAP activity upon overexpression of PA287 $(0.02 \mu g/mL \text{ tetracycline})$ (Figure 5) were further investigated to evaluate tTA expression. Overexpression of PA28y did not significantly affect tTA levels in cells cultured in the absence of tetracycline, but resulted in a 22% decrease in tTA levels in cells cultured in the presence of tetracycline as determined by monitoring iRFP fluorescence (Figure S5, *p < 0.05), suggesting that UPS activation in the presence of tetracycline results in a decrease in tTA self-amplification.

These findings suggest that, as predicted by the mathematical model, the Hys-Deg circuit is a sensor of proteasomal degradation and can be tuned with tetracycline to detect desired changes in UPS activity.

Modulating the Hysteretic Response of the Hys-Deg. To investigate whether the hysteretic behavior of the Hys-Deg circuit is determined by the ratio of constitutively expressed to inducible tTA as indicated by the modeling results, we investigated the response of the Hys-Deg circuit based on different α_{CMV}/β_{TRE} ratios to tetracycline dosage. Because tTA and iRFP are expressed cocistronically, high iRFP fluorescence

correlates with a high tTA expression level, corresponding to the OFF state of the system, while low iRFP fluorescence correlates with a low tTA expression level, corresponding to the ON state of the system. HEK293T/Hys cells were cultured in the absence of tetracycline for 4 days to equilibrate the system at the OFF state or in the presence of tetracycline (1 μ g/mL) for 4 days to equilibrate the system at the ON state. An incubation time of 4 days was adequate to switch the system from OFF to ON (Figure S6). Cells were then reseeded and cultured in the presence of increasing tetracycline concentrations (0–1 μ g/mL). When the cells were preset at the OFF state, the iRFP fluorescence intensity decreased as a function of tetracycline concentration (Figure 6), whereas SEAP activity increased as a function of tetracycline

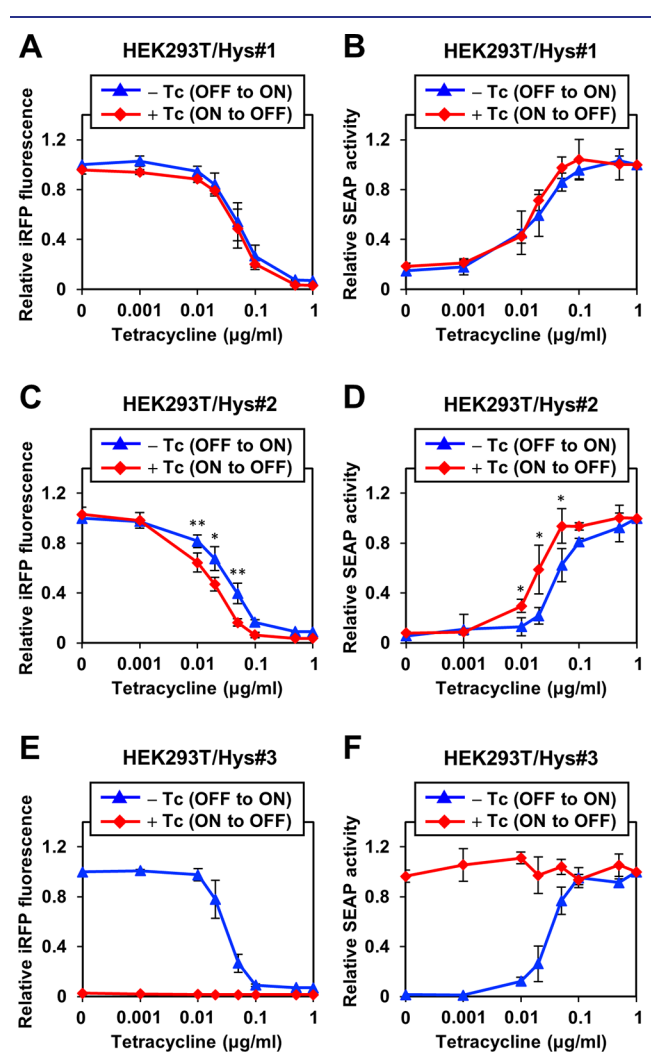


Figure 6. Hysteretic behavior of the Hys-Deg system. iRFP fluorescence and SEAP expression levels of (A, B) HEK293T/Hys#1, (C, D) HEK293T/Hys#2, and (E, F) HEK293T/Hys#3 cells cultured in the absence and presence of tetracycline (1 μ g/mL) for 4 days to set SEAP expression to an OFF (-Tc) or ON (+Tc) state and reseeded and cultured with increasing concentrations of tetracycline (0-1 μ g/mL) for 4 days. Relative iRFP fluorescence values were calculated by normalizing the iRFP fluorescence intensity of each sample to that of cells cultured in the absence of tetracycline (maximum iRFP fluorescence intensity). Relative SEAP activity values were calculated by normalizing the SEAP activity of each sample to that of cells treated with 1 μ g/mL tetracycline (maximum SEAP activity). All data are presented as mean \pm s.d. ($n \ge 3$).

concentration. All three HEK293T/Hys clones required 0.1 μg/mL of tetracycline to turn SEAP expression from OFF to ON (Figure 6). When the cells were preset at the ON state, iRFP fluorescence intensity (Figure 6A) and SEAP activity (Figure 6B) of cells presenting high α_{CMV}/β_{TRE} ratio (HEK293T/Hys#1) were identical to those of cells preset at the OFF state, suggesting a graded response to tetracycline dosage. However, analysis of cells presenting an intermediate α_{CMV}/β_{TRE} ratio (HEK293T/Hys#2) revealed that tetracycline concentrations of 0.05 μ g/mL or lower are needed for the iRFP expression to be turned ON and for the SEAP expression to be turned OFF (Figure 6C,D), revealing that the output of the system is dependent on its expression history, which is characteristic of hysteresis. Interestingly, cells presenting a low α_{CMV}/β_{TRE} ratio (HEK293T/Hys#3) displayed iRFP fluorescence intensity (ranging from 1.4 to 2.6% of the maximum iRFP fluorescence intensity at the tetracycline concentrations tested) and SEAP expression level (ranging from 93.7 to 111% of the SEAP activity of cells at the ON state at the tetracycline concentrations tested) comparable to that of cells continuously cultured in the presence of 1 μ g/mL tetracycline (1.5% iRFP and 100% SEAP, Figure 6E,F), indicating that the system was maintained at the ON state even after complete removal of tetracycline. These results confirm the modeling prediction and demonstrate that the hysteretic region is a function of $lpha_{\rm CMV}/eta_{
m TRE}$ ratio, with cells presenting lower $lpha_{
m CMV}/eta_{
m TRE}$ ratio behaving hysteretically within a wider range of tetracycline concentration. Specifically, the tetracycline concentration that is required to turn the system OFF decreases with decreasing ratio of constitutive to inducible rate of tTA synthesis. Because of the very low α_{CMV}/β_{TRE} ratio, the GFP signal of HEK293T/ Hys#3 cells was virtually undetectable (Figure 4A). As a result, these cells generate an extreme hysteretic response and commit to remain at the ON state in an irreversible manner, 59 which leads to high SEAP levels after removal of tetracycline and memory of the cellular event. Simulation of the GFP of signal of a Hys-Deg circuit based on α_{CMV}/β_{TRE} = 0.00001 using the mathematical model revealed that this system exhibits memory of tetracycline induction (Figure S7), which is consistent with experimental results obtained using HEHK293T/Hys#3 cells.

To confirm that the iRFP fluorescence and SEAP expression levels observed upon cell treatment with tetracycline result from tTA self-activation and not simply from tetracyclineinduced displacement of tTA from the SEAP promoter, we evaluated GFP, iRFP, and tTA protein levels in HEK293T/ Hys cells treated with increasing concentrations of tetracycline $(0-1 \mu g/mL)$. As expected, GFP protein levels were not affected by the addition of tetracycline (Figure 7). In agreement with the results observed from the flow cytometry analyses, iRFP protein levels in cells presenting all three α_{CMV} $eta_{\it TRE}$ ratios decreased as a function of tetracycline concentration (Figure 7). tTA protein levels decreased with increasing tetracycline concentration (Figure 7), confirming that selfamplification of tTA is negatively regulated by tetracycline. Both the tTA and iRFP protein levels of cells presenting high α_{CMV}/β_{TRE} ratio decreased gradually with increase in tetracycline concentration (Figure 7A), indicating a graded response of the system to the stimulus, which is consistent with the flow cytometry and SEAP activity analyses. However, tTA and iRFP proteins of cells presenting intermediate and low α_{CMV}/β_{TRE} ratios were not detectable upon treatment with tetracycline concentration higher than 0.05 µg/mL and 0.02 μ g/mL, respectively (Figure 7B,C), consistent with flow

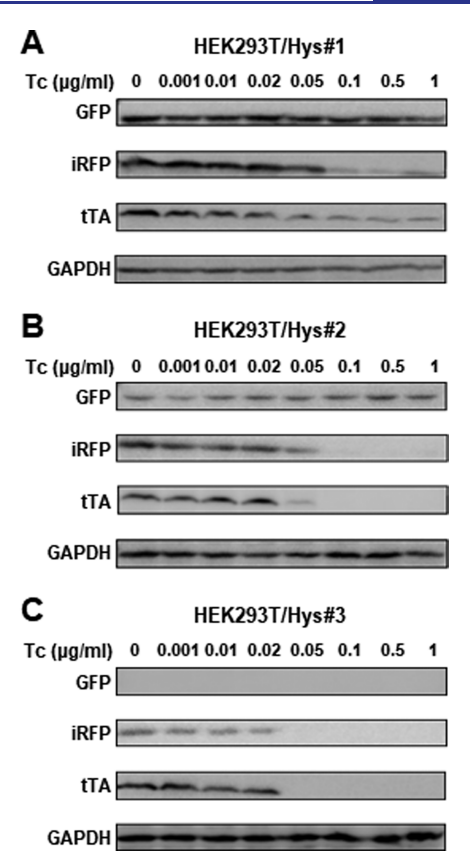


Figure 7. Analyses of protein levels of the Hys-Deg system in response to tetracycline dosage. Western blot analyses of GFP, iRFP, and tTA in (A) HEK293T/Hys#1, (B) HEK293T/Hys#2, and (C) HEK293T/Hys#3 cells cultured with increasing concentrations of tetracycline $(0-1~\mu g/mL)$ for 4 days. GAPDH was used as a loading control.

cytometry analyses showing that cells presenting intermediate and low α_{CMV}/β_{TRE} ratios present low or undetectable GFP fluorescence levels (Figure 4A). These findings confirm that tetracycline blocks self-activation of tTA.

Taken together, these results demonstrate that the hysteretic response of the Hys-Deg system can be modulated by controlling the ratio of expression of constitutive to inducible tTA.

DISCUSSION

Advances in mammalian synthetic biology have generated new tools to study cellular signal processing circuits 60-63 and opened the way to the design of engineered cells with controlled behaviors. In this study, we address the need for engineering tools that can be used in the context of the sophisticated homeostatic mechanisms of mammalian cells.²¹ This innate homeostatic system is often the main roadblock to the development of cell-based devices for the detection of transient biological behaviors. Not surprisingly, establishing robust synthetic gene circuits that provide sustained responses to transient perturbations has become a challenge in the mammalian synthetic biology field. This study investigates the design rules of a device with cellular memory, which enables conversion of a transient perturbation into a lasting response. For instance, synthetic memory modules could dramatically improve the detection of disease signatures and would make it possible to achieve sustained production of recombinant

proteins without using large quantities of inducers. ^{22,23} A number of genetic circuits engineered from transcription-based parts combined to generate a variety of different topologies have been investigated to determine whether a given topology presents cellular memory. ^{26–28,31,36,64,65} The construction of programmable memory devices is currently limited by the lack of design rules for building hysteretic circuits and a detailed understanding of the parameters that govern hysteretic behaviors. ³⁵

Enhancement of UPS activity is considered a promising therapeutic strategy for the treatment of protein misfolding diseases. 40-42 Efficient detection of proteasomal activation requires the use of a cellular device that records transient changes in UPS activity, thus enabling high throughput interrogation of chemical and genetic activators that may affect the degradation machinery with different kinetics. To establish the design rules of programmable synthetic networks with cellular memory, we developed a genetic circuit for detection of proteasomal degradation based on a positive feedback loop. To construct the positive feedback loop, we used previously characterized components of the Tet regulatory system, namely tTA and the tetracycline-inducible promoter. tTA was engineered to interface with the proteasomal degradation machinery by fusion to the ODC degron tag, resulting in an engineered tTA variant that is sensitive to changes in UPS activity. Expression of tTA was controlled by the tetracycline-inducible promoter, generating a self-activation loop (Figure 1). The circuit included a second tTA gene that is constitutively expressed and triggers the selfactivation loop. In this study, we demonstrated that a single self-activation loop can endow regulatory networks with tunable hysteresis. On the basis of mathematical modeling, we predicted and experimentally verified that the hysteresis region can be tuned by manipulating the ratio of expression of constitutive to inducible tTA (α_{CMV}/β_{TRE}). While the system presenting a high α_{CMV}/β_{TRE} ratio displayed a graded response to a stimulus, the system presenting an intermediate $\alpha_{\text{CMV}}/\beta_{\text{TRE}}$ ratio exhibited a hysteretic response to a transient stimulus.

The hysteretic behavior of the Hys-Deg system could be enhanced by further decreasing the α_{CMV}/β_{TRE} ratio, leading to an irreversible response and generating long-term memory in response to a brief pulse of induction. Previous studies have shown that hysteresis of a synthetic circuit can be achieved by altering intrinsic parameters of the circuit's components, such as cooperativity and DNA binding affinity, 25,66 which would require extensive protein engineering. This study, on the other hand, provides a universal strategy to easily and predictably control hysteretic responses by modulating the expression level of relevant circuit components. We anticipate that the hysteretic behavior could be further optimized by engineering the circuit component driving the self-activation loop (i.e., tTA) through the use of stronger activation domains. 67 Using stronger activators will give rise to a more robust positive feedback loop, and thus potentially allow for a wider range of tunable hysteresis.

In this study, tTA was rewired as a substrate of proteasomal degradation by fusion to a representative degradation tag, the ODC degron tag, which interfaces with a ubiquitin-independent pathway mediating proteasomal degradation, to allow for detection of UPS activation. Owing to the modular nature of the degradation tag, 34 the Hys-Deg circuit can also be adapted to detect proteasomal degradation arising from alternative pathways, such as the ubiquitin-dependent

proteasomal degradation.⁶⁸ Moreover, we anticipate that by customizing the signaling unit fused to tTA with respect to the interfacing cellular circuitry, the hysteretic genetic circuit can be a plug-and-play platform to detect perturbations in other signaling pathways, which will potentially advance our understanding of mechanisms underlying other important cellular responses.

In summary, we combined mathematical modeling and experimental tests to establish the design rules for constructing a hysteretic genetic circuit with an autoregulatory feedback loop. The Hys-Deg system provides a tunable technology for detection of proteasomal degradation. By providing cellular memory of a transient stimulus, this synthetic gene circuit could be easily integrated into more complex networks and enable the analysis and engineering of highly dynamic processes in mammalian cells.

MATERIALS AND METHODS

Plasmids. PCR amplifications of DNA fragments smaller than 2000 bp were performed using Vent DNA polymerase (New England Biolabs), while PCR amplifications of DNA fragments larger than 2000 bp were performed using KAPA HiFi HotStart DNA polymerase (KAPA Biosystems), according to the manufacturer's protocol. Plasmid sequences were verified using Sanger sequencing.

The plasmid pTO_SEAP was generated by replacing the GFP gene of pTO GFP³⁴ with the SEAP gene amplified from pDRIVESSEAP-hHSP70 (InvivoGen), using restriction enzymes KpnI-HF and EcoRI-HF (New England Biolabs). The plasmid pLenti CMV tTA was constructed by first generating the vector backbone by replacing the SV40 promoter and blasticidin-resistance gene of pLenti CMV_GFP Blast (Addgene plasmid #17445) with a cassette comprising the $EF1\alpha$ promoter, ⁶⁹ and the hygromycin-resistance gene⁷⁰ using Gibson Assembly. A cassette comprising an IRES (internal ribosome entry site) sequence amplified from pMSCV PIG (Addgene plasmid#21654) and the gene encoding tTA-ODC amplified from pTRE tTA³⁴ was inserted downstream of the gene encoding GFP using BsrGI-HF and SalI-HF, generating pLenti CMV tTA. pLenti TRE tTA was generated by replacing the CMV/TO eGFP cassette of pLenti CMV/ TO eGFP Puro (Addgene plasmid#17481) with a sequence consisting of the TRE promoter (comprising seven repeats of the 19bp TO sequence and the minimal CMV promoter), the gene encoding tTA-ODC, an IRES amplified from pMSCV PIG, and the gene encoding iRFP amplified from piRFP (Addgene plasmid#31857). The cassette containing the TRE promoter and tTA-ODC was amplified from pTRE_tTA³⁴ and cloned into the lentiviral vector pLenti CMV/TO eGFP Puro via Gibson Assembly ⁷¹ using the Gibson Assembly Master Mix (New England Biolabs) according to the manufacturer's protocol. The gene encoding the V5 tag was fused to the 3' of iRFP by reverse primer extension PCR. The plasmid pPA28 encoding the proteasome activator subunit PA28y was generated as previously described.³⁴

DNA sequences of circuits components used in this study are provided in Supplementary Table 2.

Cell Cultures and Transfection. HEK293T cells (ATCC) and HEK293T cells stably expressing the hysteretic genetic circuit (HEK293T/Hys) were cultured in high glucose DMEM (Hyclone) supplemented with 10% fetal bovine serum (FBS, Sigma) and 1% penicillin–streptomycin–glutamine (PSQ, Hyclone) at 37 °C in humidified 5% CO₂ atmosphere.

Cells were transfected using JetPrime (Polyplus transfection) according to the manufacturer's protocol.

Lentiviral Vector Production and Transduction. HEK293T cells were seeded in 10 cm culture dishes (1.5 × 10⁶ cells per dish) 24 h prior to transfection. Cells were cotransfected using JetPrime with a total of 5 μ g plasmid DNA: 0.8 µg of lentivirus construct (pLenti CMV tTA or pLenti TRE tTA), 2 µg of lentivirus packaging plasmid pMDLg/ pRRE (Addgene plasmid #12251), 1 µg of Rev expressing plasmid pRSV-Rev (Addgene plasmid #12253), and 1.2 µg of envelope expressing plasmid pMD2.g (Addgene plasmid #12259).^{72,73} The medium was replaced 8 h post-transfection. The culture supernatant was collected 48 h after transfection and filtered through a 0.45 μ m low protein-binding PVDF filter (Millipore). Lentivirus particles were concentrated with a Lenti-X Concentrator (Clontech) according to the manufacturer's protocol, resuspended in 1/100th of the original volume using complete DMEM, and stored at −80 °C.

HEK293T/SEAP and HEK293T/SEAP-TRE-tTA cells were seeded in 6-well plates (1.2×10^5 cells per well) 24 h prior to transduction. Cells were transduced with lentiviral particles at the desired multiplicity of infection (MOI) with Polybrene (Sigma) at a final concentration of 8 μ g/mL. The medium containing the virus was replaced with fresh medium 24 h post-transduction. Cells were harvested using TrypLE (GIBCO Invitrogen) 48 h post-transfection and subcultured in 10 cm culture dishes using selection medium supplemented appropriate antibiotics.

Stable Cell Lines. The HEK293T/Hys stable cell line was generated by first selecting a monoclonal population of HEK293T cells stably expressing TO_SEAP. HEK293T cells were transfected with the pTO_SEAP plasmid linearized with FspI. Transfected cells were cultured in DMEM supplemented with 10% FBS, 1% PSQ, and 200 μg/mL zeocin (InvivoGen) for 3 weeks and subcultured into 96-well plates at a concentration of 0.5 cells/well to isolate monoclonal populations. A stable monoclonal cell line expressing SEAP at the level representing the average SEAP activity of 30 clones screened (HEK293T/SEAP) was selected for subsequent transduction with lentiviral vector pLenti TRE tTA and pLenti CMV tTA. The HEK293T/SEAP cell line was first transduced with lentiviral vector pLenti TRE tTA and selected using medium supplemented with 1 μ g/mL puromycin (InvivoGen) for 3 weeks. The resulting polyclonal population (HEK293T/SEAP-TRE-tTA) was transduced with lentiviral vector pLenti CMV tTA and selected using medium supplemented with 200 µg/mL hygromycin B (Gold Biotechnology Inc.) for 3 weeks, generating a polyclonal population of cells expressing the hysteretic genetic circuit (HEK293T/Hys). The polyclonal population of HEK293T/ Hys cells was isolated using fluorescence-activated cell sorting to isolate colonies with different expression ratios of GFP (pLenti CMV tTA) to iRFP (pLenti TRE tTA).

Fluorescence-Activated Cell Sorting (FACS) and Flow Cytometry Analyses. Cell sorting was conducted using a FACSAria II flow cytometer (BD, San Jose, CA). Polyclonal HEK293T/Hys cells were collected in HEPES buffer supplemented with 1% BSA and 2 mM EDTA and sorted for populations with different ratios of fluorescence intensities of GFP (488 nm laser, 530/30 nm emission filter) to iRFP (633 nm laser, 780/60 nm emission filter). Sorted cells were collected in DMEM supplemented with 20% FBS in 96-well plates at a concentration of 1 cell/well to isolate monoclonal

colonies. Monoclonal colonies were cultured and amplified to obtain monoclonal populations.

Flow cytometry analyses were conducted using a FACS-Canto II flow cytometer (BD, San Jose, CA) to measure the fluorescence intensity of GFP (488 nm laser, 530/30 nm emission filter) and iRFP (633 nm laser, 780/60 nm emission filter). At least 20 000 cells were recorded for analysis in each sample.

Quantitative RT-PCR. Total RNA was extracted using RNeasy Plus Mini kit (Qiagen), and cDNA was synthesized using qScript cDNA SuperMix (Quanta Biosciences) according to the manufacturer's protocol. Quantitative RT-PCR reactions were performed using PerfeCTa SYBR Green FastMix (Quanta Biosciences) in a CFX96 Real-Time PCR Detection System (Bio-Rad) using corresponding primers listed in Supplementary Table 3.

SEAP Activity Assay. HEK293T/Hys cells were plated onto 12-well plates in medium supplemented with tetracycline $(0-1~\mu g/mL)$. The culture medium was replaced with fresh medium supplemented with tetracycline every 24 h. The medium was collected after 96 h, and SEAP expression was analyzed using SEAP Reporter Assay Kit (Invivogen) according to the manufacturer's protocol.

The effect of PA28 γ was tested by plating HEK293T/Hys cells into 12-well plates in medium supplemented with 0.02 μ g/mL tetracycline 24 h prior to transfection. Cells were transfected with 500 ng of pPA28 γ or pcDNA3.1 using JetPrime (Polyplus transfection) according to the manufacturer's protocol. The culture medium of transfected cells was replaced with fresh medium containing 0.02 μ g/mL tetracycline 24 h post-transfection. The medium was collected 48 h post-transfection and SEAP expression was analyzed using SEAP Reporter Assay Kit (Invivogen) according to the manufacturer's protocol.

Western Blot Analyses. Cells were lysed with Complete lysis-M buffer containing a protease inhibitor cocktail (Roche Applied Science) according to the manufacturer's protocol. Lysed cells were centrifuged for 5 min at 15 000g and 4 °C and the supernatant was collected for Western blot analyses. Protein concentrations were determined by Bradford assay, and samples were diluted to the same concentration and separated by 12% SDS-PAGE. Western blot analyses were performed using primary antibodies (anti-VP16, sc-7545, Santa Cruz Biotechnology; anti-V5, sc-83849-R, Santa Cruz Biotechnology; anti-GFP, 55423, AnaSpec Inc.; anti-GAPDH, NB300-320, Novus Biologicals) and appropriate secondary antibodies (m-IgGk BP-HRP, sc-516102, Santa Cruz Biotechnology; antirabbit IgG-HRP, sc-2357, Santa Cruz Biotechnology; antichicken IgY-HRP, sc-2428, Santa Cruz Biotechnology; antigoat IgG-HRP, sc-2020, Santa Cruz Biotechnology). Blots were visualized using SuperSignal Chemiluminescent Substrates (ThermoFisher).

Mathematical Model. A differential algebraic equation model was implemented using MATLAB (MathWorks, Inc.) to simulate SEAP production profiles and perform bifurcation analyses. Changes in the concentration of SEAP were modeled as dependent on the rate of SEAP synthesis ($R_{\rm SEAP}$), the rate of SEAP degradation ($\gamma_{\rm SEAP}$), and the cell number (N).

$$\frac{\mathrm{d[SEAP]}}{\mathrm{d}t} = R_{\mathrm{SEAP}}N - \gamma_{\mathrm{SEAP}}[\mathrm{SEAP}]$$

The rate of SEAP synthesis was described using the Hill function as previously reported, 34,56 modified to incorporate

the basal expression of SEAP due to promoter leakage⁷⁴ and to account for residual binding of tetracycline-bound tTA to the operator,³⁴ where the parameter θ_1 accounts for the basal expression of SEAP, $\beta_{\rm SEAP}$ is the maximal synthesis rate of SEAP, $[tTA^*]$ is the concentration of free tTA, [tTA - Tc] is the concentration of tetracycline-bound tTA, $n_{\rm R}$ is the degree of cooperativity of repression, and $K_{\rm R}$ and $K_{\rm R}'$ are the dissociation constants of tTA and tTA-Tc binding to the CMV/TO promoter, respectively. μ is the cell growth rate.

$$R_{\text{SEAP}} = \beta_{\text{SEAP}} \left(\theta_1 + (1 - \theta_1) \frac{1}{1 + \left(\frac{[tTA^*]}{K_R}\right)^{n_R} + \left(\frac{[tTA - Tc]}{K_{R_{\prime}}}\right)^{n_R}} \right)$$

$$\frac{dN}{dt} = \mu N$$

Changes in the concentration of tTA were modeled as depending on the rate of tTA synthesis ($R_{\rm tTA}$), which includes tTA that is constitutively expressed by the *CMV* promoter (α_{CMV}) modified by the translation coefficient of protein translated after the IRES, f) and tTA that is induced by tTA binding to the *TRE* promoter, the rate of degradation (γ_{tTA}), and dilution due to cell growth (μ). The rate of tTA synthesis controlled by the *TRE* promoter is described using the Hill function, for which the parameter θ_2 accounts for the basal expression of tTA, β_{TRE} is the maximal synthesis rate of tTA controlled by the *TRE* promoter, [tTA*] is the concentration of free tTA, [tTA - Tc] is the concentration of tetracycline-bound tTA, n_A is the degree of cooperativity of activation, and K_A and $K_{A'}$ are the dissociation constants of tTA and tTA—Tc binding to the *TRE* promoter, respectively.

$$\frac{\mathrm{d[tTA]}}{\mathrm{d}t} = R_{\mathrm{tTA}} - (\gamma_{\mathrm{tTA}} + \mu)[\mathrm{tTA}]$$

$$R_{\text{tTA}} = f\alpha_{CMV} + \beta_{TRE} \left(\theta_2 + (1 - \theta_2) \frac{\left(\frac{[\text{tTA}^*]}{K_A} \right)^{n_A} + \left(\frac{[\text{tTA} - \text{Tc}]}{K_{A_s}} \right)^{n_A}}{1 + \left(\frac{[\text{tTA}^*]}{K_A} \right)^{n_A} + \left(\frac{[\text{tTA} - \text{Tc}]}{K_{A_s}} \right)^{n_A}} \right)$$

The binding of tetracycline to tTA was also modeled using the Hill function, 47 where [tTA] is the total cellular tTA concentration, [Tc] is the concentration of tetracycline, n_{Tc} is the Hill coefficient of tetracycline binding to tTA, and K_{Tc} is the dissociation constant of tetracycline binding to tTA.

$$\frac{[tTA^*]}{[tTA]} = \frac{1}{1 + \left(\frac{[Tc]}{K_{Tc}}\right)^{n_{Tc}}}$$

$$[tTA] = [tTA^*] + [tTA - Tc]$$

The relative SEAP expression ([SEAP]_{norm}) was obtained by normalizing the SEAP production obtained 24 h after tTA expression reaches steady state ([SEAP]) to the SEAP production obtained 24 h after tTA expression reaches steady state when tetracycline is in great excess ([SEAP]_{max}).

$$[SEAP]_{norm} = \frac{[SEAP]}{[SEAP]_{max}}$$

The parameter values for all simulations are provided in Supplementary Table 1.

Statistical Analyses. All data are presented as mean \pm s.d or mean \pm s.e.m. ($n \ge 3$ biological replicates). Statistical significance was calculated using a two-tailed t test in all experiments.

ASSOCIATED CONTENT

S Supporting Information

The Supporting Information is available free of charge on the ACS Publications website at DOI: 10.1021/acssynbio.9b00074.

Parameters used for the mathematical model; nucleotide sequences of the circuit components; primers used for quantitative RT-PCR experiments; additional figures supporting the main text (PDF)

AUTHOR INFORMATION

Corresponding Author

*E-mail: segatori@rice.edu.

ORCID ®

Laura Segatori: 0000-0001-5749-5479

Author Contributions

Y.Z., W.Z., and L.S. conceived the project. Y.Z. and L.S. designed the experiments and analyzed the results. Y.Z. and T.N. executed the experiments. Y.Z. and L.S. wrote the manuscript. Y.Z., B.B., and L.S. revised the manuscript.

Notes

The authors declare no competing financial interest.

ACKNOWLEDGMENTS

This work was funded by the National Science Foundation (MCB-1615562 and 1150138, and CBET 1805317) and the Welch Foundation (C-1824).

REFERENCES

- (1) Weber, W., and Fussenegger, M. (2012) Emerging biomedical applications of synthetic biology. *Nat. Rev. Genet.* 13, 21–35.
- (2) Kilpatrick, K., Zeng, Y., Hancock, T., and Segatori, L. (2015) Genetic and chemical activation of TFEB mediates clearance of aggregated α-synuclein. *PLoS One 10*, No. e0120819.
- (3) Mohan, C., Kim, Y. G., Koo, J., and Lee, G. M. (2008) Assessment of cell engineering strategies for improved therapeutic protein production in CHO cells. *Biotechnol. J.* 3, 624–630.
- (4) Andersen, D. C., and Reilly, D. E. (2004) Production technologies for monoclonal antibodies and their fragments. *Curr. Opin. Biotechnol.* 15, 456–462.
- (5) Chu, L., and Robinson, D. K. (2001) Industrial choices for protein production by large-scale cell culture. *Curr. Opin. Biotechnol.* 12, 180–187.
- (6) Geall, A. J., Mandl, C. W., and Ulmer, J. B. (2013) RNA: The new revolution in nucleic acid vaccines. *Semin. Immunol.* 25, 152–159.
- (7) Sharma, A. R., Kundu, S. K., Nam, J. S., Sharma, G., Doss, C. G. P., Lee, S. S., and Chakraborty, C. (2014) Next generation delivery system for proteins and genes of therapeutic purpose: Why and how? *Biomed Res. Int. 2014*, No. No. 327950, DOI: 10.1155/2014/327950.
- (8) Mathur, M., Xiang, J. S., and Smolke, C. D. (2017) Mammalian synthetic biology for studying the cell. *J. Cell Biol.* 216, 73–82.
- (9) Brandman, O., and Meyer, T. (2008) Feedback Loops Shape Cellular Signals in Space and Time. *Science* 322, 390–396.
- (10) Song, W., Soo Lee, S., Savini, M., Popp, L., Colvin, V. L., and Segatori, L. (2014) Ceria nanoparticles stabilized by organic surface coatings activate the lysosome-autophagy system and enhance autophagic clearance. *ACS Nano* 8, 10328–10342.

(11) Zhao, W., Pferdehirt, L., and Segatori, L. (2018) Quantitatively predictable control of cellular protein levels through proteasomal degradation. *ACS Synth. Biol.* 7, 540–552.

- (12) Kobayashi, H., Kaern, M., Araki, M., Chung, K., Gardner, T. S., Cantor, C. R., and Collins, J. J. (2004) Programmable cells: interfacing natural and engineered gene networks. *Proc. Natl. Acad. Sci. U. S. A. 101*, 8414–8419.
- (13) O'Shaughnessy, E. C., Palani, S., Collins, J. J., and Sarkar, C. A. (2011) Tunable signal processing in synthetic MAP kinase cascades. *Cell* 144, 119–131.
- (14) Bintu, L., Yong, J., Antebi, Y. E., McCue, K., Kazuki, Y., Uno, N., Oshimura, M., and Elowitz, M. B. (2016) Dynamics of epigenetic regulation at the single-cell level. *Science* 351, 720–724.
- (15) Atkinson, M. R., Savageau, M. A., Myers, J. T., and Ninfa, A. J. (2003) Development of genetic circuitry exhibiting toggle switch or oscillatory behavior in Escherichia coli. *Cell* 113, 597–607.
- (16) Pedraza, J. M., and van Oudenaarden, A. (2005) Noise propagation in gene networks. *Science* 307, 1965–1969.
- (17) Pu, J., Zinkus-Boltz, J., and Dickinson, B. C. (2017) Evolution of a split RNA polymerase as a versatile biosensor platform. *Nat. Chem. Biol.* 13, 432–438.
- (18) Zeng, Y., Jones, A. M., Thomas, E. E., Nassif, B., Silberg, J. J., and Segatori, L. (2018) A split transcriptional repressor that links protein solubility to an orthogonal genetic circuit. *ACS Synth. Biol.* 7, 2126–2138
- (19) Martin, V. J. J., Pitera, D. J., Withers, S. T., Newman, J. D., and Keasling, J. D. (2003) Engineering a mevalonate pathway in Escherichia coli for production of terpenoids. *Nat. Biotechnol.* 21, 796–802.
- (20) Walter, P., and Ron, D. (2011) The unfolded protein response: from stress pathway to homeostatic regulation. *Science* 334, 1081–1086
- (21) Koga, H., Kaushik, S., and Cuervo, A. M. (2011) Protein homeostasis and aging: The importance of exquisite quality control. *Ageing Res. Rev.* 10, 205–215.
- (22) Inniss, M. C., and Silver, P. A. (2013) Building synthetic memory. Curr. Biol. 23, R812–R816.
- (23) Burrill, D. R., and Silver, P. A. (2010) Making cellular memories. *Cell* 140, 13–18.
- (24) Markevich, N. I., Hoek, J. B., and Kholodenko, B. N. (2004) Signaling switches and bistability arising from multisite phosphorylation in protein kinase cascades. *J. Cell Biol.* 164, 353–359.
- (25) Shopera, T., Henson, W. R., Ng, A., Lee, Y. J., Ng, K., and Moon, T. S. (2015) Robust, tunable genetic memory from protein sequestration combined with positive feedback. *Nucleic Acids Res.* 43, 9086–9094.
- (26) May, T., Eccleston, L., Herrmann, S., Hauser, H., Goncalves, J., and Wirth, D. (2008) Bimodal and hysteretic expression in mamalian cells from a synthetic gene circuit. *PLoS One* 3, No. e2372.
- (27) Becskei, a, Séraphin, B., and Serrano, L. (2001) Positive feedback in eukaryotic gene networks: cell differentiation by graded to binary response conversion. *EMBO J.* 20, 2528–2535.
- (28) Gardner, T. S., Cantor, C. R., and Collins, J. J. (2000) Construction of a genetic toggle switch in Escherichia coli. *Nature* 403, 339-42.
- (29) Shen-Orr, S. S., Milo, R., Mangan, S., and Alon, U. (2002) Network motifs in the transcriptional regulation network of Escherichia coli. *Nat. Genet.* 31, 64–68.
- (30) Lee, T. I., Rinaldi, N. J., Robert, F., Odom, D. T., Bar-Joseph, Z., Gerber, G. K., Hannett, N. M., Harbison, C. T., Thompson, C. M., Simon, I., Zeitlinger, J., Jennings, E. G., Murray, H. L., Gordon, D. B., Ren, B., Wyrick, J. J., Tagne, J.-B., Volkert, T. L., Fraenkel, E., Gifford, D. K., and Young, R. A. (2002) Transcriptional regulatory networks in Saccharomyces cerevisiae. *Science* 298, 799–804.
- (31) Kramer, B. P., Viretta, A. U., Daoud-El-Baba, M., Aubel, D., Weber, W., and Fussenegger, M. (2004) An engineered epigenetic transgene switch in mammalian cells. *Nat. Biotechnol.* 22, 867–870.

(32) Guido, N. J., Wang, X., Adalsteinsson, D., McMillen, D., Hasty, J., Cantor, C. R., Elston, T. C., and Collins, J. J. (2006) A bottom-up approach to gene regulation. *Nature* 439, 856–860.

- (33) Sayut, D. J., Niu, Y., and Sun, L. (2006) Construction and engineering of positive feedback loops. ACS Chem. Biol. 1, 692-696.
- (34) Zhao, W., Bonem, M., McWhite, C., Silberg, J. J., and Segatori, L. (2014) Sensitive detection of proteasomal activation using the Deg-On mammalian synthetic gene circuit. *Nat. Commun.* 5, 3612.
- (35) Chang, D.-E., Leung, S., Atkinson, M. R., Reifler, A., Forger, D., and Ninfa, A. J. (2010) Building biological memory by linking positive feedback loops. *Proc. Natl. Acad. Sci. U. S. A. 107*, 175–180.
- (36) Kramer, B. P., and Fussenegger, M. (2005) Hysteresis in a synthetic mammalian gene network. *Proc. Natl. Acad. Sci. U. S. A. 102*, 9517–9522.
- (37) Angeli, D., Ferrell, J. E., and Sontag, E. D. (2004) Detection of multistability, bifurcations, hysteresis in a large class of biological positive-feedback systems. *Proc. Natl. Acad. Sci. U. S. A. 101*, 1822–1827
- (38) Craciun, G., Tang, Y., and Feinberg, M. (2006) Understanding bistability in complex enzyme-driven reaction networks. *Proc. Natl. Acad. Sci. U. S. A.* 103, 8697–8702.
- (39) Nandi, D., Tahiliani, P., Kumar, A., and Chandu, D. (2006) The ubiquitin-proteasome system. *J. Biosci.* 31, 137–155.
- (40) Li, J., Powell, S. R., and Wang, X. (2011) Enhancement of proteasome function by PA28 α overexpression protects against oxidative stress. FASEB J. 25, 883–93.
- (41) Tonoki, A., Kuranaga, E., Tomioka, T., Hamazaki, J., Murata, S., Tanaka, K., and Miura, M. (2009) Genetic Evidence Linking Age-Dependent Attenuation of the 26S Proteasome with the Aging Process. *Mol. Cell. Biol.* 29, 1095–1106.
- (42) Vilchez, D., Boyer, L., Morantte, I., Lutz, M., Merkwirth, C., Joyce, D., Spencer, B., Page, L., Masliah, E., Travis Berggren, W., Gage, F. H., and Dillin, A. (2012) Increased proteasome activity in human embryonic stem cells is regulated by PSMD11. *Nature 489*, 304–308.
- (43) Melvin, A. T., Woss, G. S., Park, J. H., Waters, M. L., and Allbritton, N. L. (2013) Measuring activity in the ubiquitin-proteasome system: From large scale discoveries to single cells analysis. *Cell Biochem. Biophys.* 67, 75–89.
- (44) Dantuma, N. P., Lindsten, K., Glas, R., Jellne, M., and Masucci, M. G. (2000) Short-lived green fluorescent proteins for quantifying ubiquitin/proteasome-dependent proteolysis in living cells. *Nat. Biotechnol.* 18, 538–43.
- (45) Gossen, M., and Bujard, H. (1992) Tight control of gene expression in mammalian cells by tetracycline-responsive promoters. *Proc. Natl. Acad. Sci. U. S. A.* 89, 5547–5551.
- (46) Kim, H. J., Gatz, C., Hillen, W., and Jones, T. R. (1995) Tetracycline repressor-regulated gene repression in recombinant human cytomegalovirus. *J. Virol.* 69, 2565–73.
- (47) Tigges, M., Marquez-Lago, T. T., Stelling, J., and Fussenegger, M. (2009) A tunable synthetic mammalian oscillator. *Nature* 457, 309–312.
- (48) Jang, S. K., Kräusslich, H. G., Nicklin, M. J., Duke, G. M., Palmenberg, A. C., and Wimmer, E. (1988) A segment of the 5' nontranslated region of encephalomyocarditis virus RNA directs internal entry of ribosomes during in vitro translation. *J. Virol.* 62, 2636–43.
- (49) Li, X., Zhao, X., Fang, Y., Jiang, X., Duong, T., Fan, C., Huang, C., and Kain, S. R. (1998) Generation of destabilized green fluorescent protein as a transcription reporter. *J. Biol. Chem.* 273, 34970–34975.
- (50) Matsuzawa, S. -i., Cuddy, M., Fukushima, T., and Reed, J. C. (2005) Method for targeting protein destruction by using a ubiquitin-independent, proteasome-mediated degradation pathway. *Proc. Natl. Acad. Sci. U. S. A.* 102, 14982–14987.
- (51) Weber, W., Stelling, J., Rimann, M., Keller, B., Daoud-El Baba, M., Weber, C. C., Aubel, D., and Fussenegger, M. (2007) A synthetic time-delay circuit in mammalian cells and mice. *Proc. Natl. Acad. Sci. U. S. A. 104*, 2643–2648.

(52) Nevozhay, D., Adams, R. M., Murphy, K. F., Josic, K., and Balazsi, G. (2009) Negative autoregulation linearizes the dose response and suppresses the heterogeneity of gene expression. *Proc. Natl. Acad. Sci. U. S. A. 106*, 5123–5128.

- (53) Corish, P., and Tyler-Smith, C. (1999) Attenuation of green fluorescent protein half-life in mammalian cells. *Protein Eng., Des. Sel.* 12, 1035–1040.
- (54) Filonov, G. S., Piatkevich, K. D., Ting, L. M., Zhang, J., Kim, K., and Verkhusha, V. V. (2011) Bright and stable near-infrared fluorescent protein for in vivo imaging. *Nat. Biotechnol.* 29, 757–761.
- (55) Argast, M., and Beck, C. F. (1984) Tetracycline diffusion through phospholipid bilayers and binding to phospholipids. *Antimicrob. Agents Chemother.* 26, 263–265.
- (56) Rosenfeld, N., Young, J. W., Alon, U., Swain, P. S., and Elowitz, M. B. (2005) Gene regulation at the single-cell level. *Science* 307, 1962–1965.
- (57) Campeau, E., Ruhl, V. E., Rodier, F., Smith, C. L., Rahmberg, B. L., Fuss, J. O., Campisi, J., Yaswen, P., Cooper, P. K., and Kaufman, P. D. (2009) A versatile viral system for expression and depletion of proteins in mammalian cells. *PLoS One 4*, No. e6529.
- (58) Seo, H., Sonntag, K.-C., Kim, W., Cattaneo, E., and Isacson, O. (2007) Proteasome activator enhances survival of Huntington's disease neuronal model cells. *PLoS One 2*, No. e238.
- (59) Xiong, W., and Ferrell, J. E. J. (2003) A positive-feedback-based bistable 'memory module' that governs a cell fate decision. *Nature* 426, 460–465.
- (60) Win, M. N., and Smolke, C. D. (2008) Higher-order cellular information processing with synthetic RNA devices. *Science* 322, 456–461.
- (61) Xie, Z., Wroblewska, L., Prochazka, L., Weiss, R., and Benenson, Y. (2011) Multi-input RNAi-based logic circuit for identification of specific cancer cells. *Science* 333, 1307–11.
- (62) Regot, S., Hughey, J. J., Bajar, B. T., Carrasco, S., and Covert, M. W. (2014) High-sensitivity measurements of multiple kinase activities in live single cells. *Cell* 157, 1724–1734.
- (63) Ryu, J., and Park, S. H. (2015) Simple synthetic protein scaffolds can create adjustable artificial MAPK circuits in yeast and mammalian cells. *Sci. Signaling 8*, No. ra66.
- (64) Isaacs, F. J., Hasty, J., Cantor, C. R., and Collins, J. J. (2003) Prediction and measurement of an autoregulatory genetic module. *Proc. Natl. Acad. Sci. U. S. A. 100*, 7714–7719.
- (65) Ajo-Franklin, C. M., Drubin, D. A., Eskin, J. A., Gee, E. P. S., Landgraf, D., Phillips, I., and Silver, P. A. (2007) Rational design of memory in eukaryotic cells. *Genes Dev.* 21, 2271–2276.
- (66) Helbl, V., and Hillen, W. (1998) Stepwise selection of TetR variants recognizing tet operator 4C with high affinity and specificity. *J. Mol. Biol.* 276, 313–318.
- (67) Chavez, A., Scheiman, J., Vora, S., Pruitt, B. W., Tuttle, M., P R Iyer, E., Lin, S., Kiani, S., Guzman, C. D., Wiegand, D. J., Ter-Ovanesyan, D., Braff, J. L., Davidsohn, N., Housden, B. E., Perrimon, N., Weiss, R., Aach, J., Collins, J. J., and Church, G. M. (2015) Highly efficient Cas9-mediated transcriptional programming. *Nat. Methods* 12, 326–328.
- (68) Grilly, C., Stricker, J., Pang, W. L., Bennett, M. R., and Hasty, J. (2007) A synthetic gene network for tuning protein degradation in Saccharomyces cerevisiae. *Mol. Syst. Biol.* 3, 127.
- (69) Ferreira, J. P., Peacock, R. W. S., Lawhorn, I. E. B., and Wang, C. L. (2011) Modulating ectopic gene expression levels by using retroviral vectors equipped with synthetic promoters. *Syst. Synth. Biol.* 5, 131–138.
- (70) Tulu, U. S., Rusan, N. M., and Wadsworth, P. (2003) Peripheral, non-centrosome-associated microtubules contribute to spindle formation in centrosome-containing cells. *Curr. Biol.* 13, 1894–1899.
- (71) Gibson, D. G, Young, L., Chuang, R.-Y., Venter, J C., Hutchison, C. A, and Smith, H. O (2009) Enzymatic assembly of DNA molecules up to several hundred kilobases. *Nat. Methods* 6, 12–16.

(72) Dull, T., Zufferey, R., Kelly, M., Mandel, R. J., Nguyen, M., Trono, D., and Naldini, L. (1998) A third-generation lentivirus vector with a conditional packaging system. *J. Virol.* 72, 8463–8471.

- (73) Sastry, L., Johnson, T., Hobson, M. J., Smucker, B., and Cornetta, K. (2002) Titering lentiviral vectors: comparison of DNA, RNA and marker expression methods. *Gene Ther. 9*, 1155–1162.
- (74) Nevozhay, D., Zal, T., and Balázsi, G. (2013) Transferring a synthetic gene circuit from yeast to mammalian cells. *Nat. Commun. 4*, 1451.